Proto-neutron star in generalized thermo-statistics

K. Miyazaki

E-mail: miyazakiro@rio.odn.ne.jp

Abstract

The proto-neutron star (PNS) is investigated for the first time in the generalized thermo-statistics. The subextensive entropy for the power-law index $q > 1$ leads to much lower temperature in a core of PNS than the Clausius extensive entropy. Consequently, we can see a clear difference between the mass-radius relation of PNS in the standard ($q = 1.0$) and generalized ($q = 1.3$) thermo-statistics. The result is essentially due to the effect of gravitation that is consistent with the subextensivity of the generalized entropy.

A proto-neutron star (PNS) [1,2] is born during 0.1-1s after the core bounce of successful supernova explosion. The PNS is a hot and lepton-rich object and so is quite different from the ordinary neutron star (NS) observed as a radio pulsar. It is composed of a shocked envelope and an un-shocked core of entropy per baryon $S \sim 1$. The core is in quasi-stationary β-equilibrium state because the time scale of weak interaction is much shorter than the time scale of neutrino diffusion. We can therefore study an equation-of-state (EOS) of PNS in the nuclear physics of dense baryon matter. So far the EOS of PNS has been investigated [3-10] within the standard Boltzmann-Gibbs thermo-statistics. To the contrary the present paper calculates the EOS for the first time within the generalized thermo-statistics [11-13]. We make use of the relativistic mean-field (RMF) model of PNS matter developed in Ref. [14]. The RMF model is reasonable because the investigation of PNS needs the general relativity that is based on the validity of the special relativity at local space-time, where the microscopic nuclear model is developed.

We extend the thermodynamic potential in Ref. [14] using the q-deformed exponential and logarithm [15]:

$$\exp_q(x) \equiv \left[\, 1 + (1-q)\, x \,\right]^{1/(1-q)} , \tag{1}$$

$$\ln_q(x) \equiv \frac{x^{1-q} - 1}{1-q}. \tag{2}$$

Consequently, the thermodynamic potential Ω_q in the generalized thermo-statistics is

$$\begin{aligned}\Omega_q &= \frac{1}{2}\,m_\sigma^2\,\langle\sigma\rangle^2+\frac{1}{2}\,m_\delta^2\,\langle\delta_3\rangle^2+\frac{1}{2}\,m_{\sigma^*}^2\,\langle\sigma^*\rangle^2-\frac{1}{2}\,m_\omega^2\,\langle\omega_0\rangle^2-\frac{1}{2}\,m_\rho^2\,\langle\rho_{03}\rangle^2-\frac{1}{2}\,m_\phi^2\,\langle\phi_0\rangle^2\\
&-2\,k_B\,T\sum_{\substack{B=p,n,\Lambda,\Sigma^+,\\ \Sigma^0,\Sigma^-,\Xi^0,\Xi^-}}\int\frac{d^3\mathbf{k}}{(2\pi)^3}\left\{\ln_q\left[1+\exp_q\left(\frac{\nu_B-E^*_{kB}}{k_BT}\right)\right]\right.\\
&\qquad\left.+\ \ln_q\left[1+\exp_q\left(\frac{-\nu_B-E^*_{kB}}{k_BT}\right)\right]\right\}\\
&-k_B\,T\sum_{l=e^-,\mu^-,\nu_e,\nu_\mu}\gamma_l\int\frac{d^3\mathbf{k}}{(2\pi)^3}\left\{\ln_q\left[1+\exp_q\left(\frac{\mu_l-e_{kl}}{k_BT}\right)\right]\right.\\
&\qquad\left.+\ \ln_q\left[1+\exp_q\left(\frac{-\mu_l-e_{kl}}{k_BT}\right)\right]\right\},\end{aligned}\tag{3}$$

where k_B is the Boltzmann constant and ν_B is given by the chemical potential μ_B and the vector potential V_B of baryon as

$$\nu_B=\mu_B-V_B.\tag{4}$$

The spin degeneracy factor for leptons is $\gamma_l=\{2,2,1\}$ for $l=\{e^-,\mu^-,\nu\}$. $M^*_B=m^*_BM_B$ and $E^*_{kB}=\left(\mathbf{k}^2+{M^*_B}^2\right)^{1/2}$ are the effective mass and the energy of baryon while μ_l and $e_{kl}=\left(\mathbf{k}^2+m_l^2\right)^{1/2}$ are the chemical potential and the energy of lepton.

The scalar mean fields $\langle\sigma\rangle$, $\langle\delta_3\rangle$ and $\langle\sigma^*\rangle$ are expressed [14] in terms of three independent effective masses of p, n and Λ while the vector mean fields $\langle\omega_0\rangle$, $\langle\rho_{03}\rangle$ and $\langle\phi_0\rangle$ are expressed [14] in terms of three independent vector potentials of p, n and Λ. Then, M^*_p, M^*_n, M^*_Λ, V_p, V_n and V_Λ are determined from extremizing the thermodynamic potential Ω_q in terms of them. The results are

$$\begin{aligned}&\rho_p+\sum_{Y\neq\Lambda}\frac{g^*_{YY\omega}\,g^*_{nn\rho}+I_{3Y}\,g^*_{YY\rho}\,g^*_{nn\omega}-\left(g^*_{\Lambda\Lambda\omega}/g^*_{\Lambda\Lambda\phi}\right)g^*_{YY\phi}\,g^*_{nn\rho}}{g^*_{pp\omega}\,g^*_{nn\rho}+g^*_{nn\omega}\,g^*_{pp\rho}}\,\rho_Y\\
&-\frac{g^*_{nn\rho}\,m_\omega^2\,\langle\omega_0\rangle+g^*_{nn\omega}\,m_\rho^2\,\langle\rho_{03}\rangle-\left(g^*_{\Lambda\Lambda\omega}/g^*_{\Lambda\Lambda\phi}\right)g^*_{nn\rho}\,m_\phi^2\,\langle\phi_0\rangle}{g^*_{pp\omega}\,g^*_{nn\rho}+g^*_{nn\omega}\,g^*_{pp\rho}}=0,\end{aligned}\tag{5}$$

$$\begin{aligned}&\rho_n+\sum_{Y\neq\Lambda}\frac{g^*_{YY\omega}\,g^*_{pp\rho}-I_{3Y}\,g^*_{YY\rho}\,g^*_{pp\omega}-\left(g^*_{\Lambda\Lambda\omega}/g^*_{\Lambda\Lambda\phi}\right)g^*_{YY\phi}\,g^*_{pp\rho}}{g^*_{pp\omega}\,g^*_{nn\rho}+g^*_{nn\omega}\,g^*_{pp\rho}}\,\rho_Y\\
&-\frac{g^*_{pp\rho}\,m_\omega^2\,\langle\omega_0\rangle-g^*_{pp\omega}\,m_\rho^2\,\langle\rho_{03}\rangle-\left(g^*_{\Lambda\Lambda\omega}/g^*_{\Lambda\Lambda\phi}\right)g^*_{pp\rho}\,m_\phi^2\,\langle\phi_0\rangle}{g^*_{pp\omega}\,g^*_{nn\rho}+g^*_{nn\omega}\,g^*_{pp\rho}}=0,\end{aligned}\tag{6}$$

$$\rho_\Lambda+\sum_{Y\neq\Lambda}\frac{g^*_{YY\phi}}{g^*_{\Lambda\Lambda\phi}}\,\rho_Y-\left(\frac{m_\phi}{g^*_{\Lambda\Lambda\phi}}\right)^2\left(V_\Lambda-g^*_{\Lambda\Lambda\omega}\,\langle\omega_0\rangle\right)=0,\tag{7}$$

$$M_p\rho_{pS}+\sum_{Y\neq\Lambda}\frac{\partial\, m_Y^*}{\partial\, m_p^*}M_Y\rho_{YS}+\sum_{Y\neq\Lambda}\frac{\partial\, V_Y}{\partial\, m_p^*}\rho_Y+m_\sigma^2\left\langle\sigma\right\rangle\frac{\partial\left\langle\sigma\right\rangle}{\partial\, m_p^*}+m_\delta^2\left\langle\delta_3\right\rangle\frac{\partial\left\langle\delta_3\right\rangle}{\partial\, m_p^*}$$
$$+\,m_{\sigma^*}^2\left\langle\sigma^*\right\rangle\frac{\partial\left\langle\sigma^*\right\rangle}{\partial\, m_p^*}-m_\omega^2\left\langle\omega_0\right\rangle\frac{\partial\left\langle\omega_0\right\rangle}{\partial\, m_p^*}-m_\rho^2\left\langle\rho_{03}\right\rangle\frac{\partial\left\langle\rho_{03}\right\rangle}{\partial\, m_p^*}-m_\phi^2\left\langle\phi_0\right\rangle\frac{\partial\left\langle\phi_0\right\rangle}{\partial\, m_p^*}=0, \quad (8)$$

$$M_n\rho_{nS}+\sum_{Y\neq\Lambda}\frac{\partial\, m_Y^*}{\partial\, m_n^*}M_Y\rho_{YS}+\sum_{Y\neq\Lambda}\frac{\partial\, V_Y}{\partial\, m_n^*}\rho_Y+m_\sigma^2\left\langle\sigma\right\rangle\frac{\partial\left\langle\sigma\right\rangle}{\partial\, m_n^*}+m_\delta^2\left\langle\delta_3\right\rangle\frac{\partial\left\langle\delta_3\right\rangle}{\partial\, m_n^*}$$
$$+\,m_{\sigma^*}^2\left\langle\sigma^*\right\rangle\frac{\partial\left\langle\sigma^*\right\rangle}{\partial\, m_n^*}-m_\omega^2\left\langle\omega_0\right\rangle\frac{\partial\left\langle\omega_0\right\rangle}{\partial\, m_n^*}-m_\rho^2\left\langle\rho_{03}\right\rangle\frac{\partial\left\langle\rho_{03}\right\rangle}{\partial\, m_n^*}-m_\phi^2\left\langle\phi_0\right\rangle\frac{\partial\left\langle\phi_0\right\rangle}{\partial\, m_n^*}=0, \quad (9)$$

$$M_\Lambda\rho_{\Lambda S}+\sum_{Y\neq\Lambda}\frac{\partial\, m_Y^*}{\partial\, m_\Lambda^*}M_Y\rho_{YS}+\sum_{Y\neq\Lambda}\frac{\partial\, V_Y}{\partial\, m_\Lambda^*}\rho_Y+m_{\sigma^*}^2\left\langle\sigma^*\right\rangle\frac{\partial\left\langle\sigma^*\right\rangle}{\partial\, m_\Lambda^*}-m_\phi^2\left\langle\phi_0\right\rangle\frac{\partial\left\langle\phi_0\right\rangle}{\partial\, m_\Lambda^*}=0. \quad (10)$$

I_{3Y} is the isospin of hyperon. The effective coupling constants $g_{BB\sigma}^*$ *etc.* are given in Ref. [14]. For the free meson-baryon coupling constants $g_{BB\sigma}$ *etc.* we make use of the EZM-P model of Table 1 in Ref. [16]. The calculations of the derivatives in Eqs. (5)-(10) are tedious but straightforward tasks and so their explicit expressions are not shown.

The baryon density is defined by [15]

$$\rho_B=-\frac{\partial\,\Omega_q}{\partial\,\mu_B}=2\int\frac{d^3\mathbf{k}}{(2\pi)^3}\left[\left(n_{qB}(k)\right)^q-\left(\bar{n}_{qB}(k)\right)^q\right], \quad (11)$$

where the q-deformed Fermi-Dirac distribution functions [15] are

$$\begin{bmatrix} n_{qB}(k) \\ \bar{n}_{qB}(k)\end{bmatrix}=\begin{cases}\dfrac{1}{1+\left[1+(q-1)\,\frac{E_{kB}^*\mp\nu_B}{k_BT}\right]^{\frac{1}{q-1}}} & \text{for}\quad 1+(q-1)\,\dfrac{E_{kB}^*\mp\nu_B}{k_BT}>0 \\ 1 & \text{for}\quad 1+(q-1)\,\dfrac{E_{kB}^*\mp\nu_B}{k_BT}\leq 0\end{cases}. \quad (12)$$

The upper and lower signs are for baryon and anti-baryon, respectively. Similarly, the lepton density is defined by

$$\rho_l=-\frac{\partial\,\Omega_q}{\partial\,\mu_l}=\gamma_l\int\frac{d^3\mathbf{k}}{(2\pi)^3}\left[\left(n_{ql}(k)\right)^q-\left(\bar{n}_{ql}(k)\right)^q\right], \quad (13)$$

where

$$\begin{bmatrix} n_{ql}(k) \\ \bar{n}_{ql}(k)\end{bmatrix}=\begin{cases}\dfrac{1}{1+\left[1+(q-1)\,\frac{e_{kl}\mp\mu_l}{k_BT}\right]^{\frac{1}{q-1}}} & \text{for}\quad 1+(q-1)\,\dfrac{e_{kl}\mp\mu_l}{k_BT}>0 \\ 1 & \text{for}\quad 1+(q-1)\,\dfrac{e_{kl}\mp\mu_l}{k_BT}\leq 0\end{cases}. \quad (14)$$

The scalar density of baryon is defined [15] by

$$\rho_{BS} = 2\int \frac{d^3\mathbf{k}}{(2\pi)^3}\,\frac{M_B^*}{E_{kB}^*}\left[\left(n_{qB}\left(k\right)\right)^q + \left(\bar{n}_{qB}\left(k\right)\right)^q\right]. \tag{15}$$

The entropy is calculated [15] as

$$\begin{aligned} TS &= -T\,\frac{\partial\,\Omega_q}{\partial\,T} \\ &= \frac{1}{2}\,m_\sigma^2\left\langle\sigma\right\rangle^2 + \frac{1}{2}\,m_\delta^2\left\langle\delta_3\right\rangle^2 + \frac{1}{2}\,m_{\sigma^*}^2\left\langle\sigma^*\right\rangle^2 \\ &\quad - \frac{1}{2}\,m_\omega^2\left\langle\omega_0\right\rangle^2 - \frac{1}{2}\,m_\rho^2\left\langle\rho_{03}\right\rangle^2 - \frac{1}{2}\,m_\phi^2\left\langle\phi_0\right\rangle^2 - \Omega_q \\ &\quad - \sum_{\substack{B=p,n,\Lambda,\Sigma^+,\\ \Sigma^0,\Sigma^-,\Xi^0,\Xi^-}}\left(\mu_B - V_B\right)\rho_B + 2\sum_{\substack{B=p,n,\Lambda,\Sigma^+,\\ \Sigma^0,\Sigma^-,\Xi^0,\Xi^-}}\int\frac{d^3\mathbf{k}}{(2\pi)^3}E_{kB}^*\left[\left(n_{qB}\left(k\right)\right)^q + \left(\bar{n}_{qB}\left(k\right)\right)^q\right] \\ &\quad - \sum_{l=e^-,\mu^-,\nu_e,\nu_\mu}\mu_l\,\rho_l + \sum_{l=e^-,\mu^-,\nu_e,\nu_\mu}\gamma_l\int\frac{d^3\mathbf{k}}{(2\pi)^3}\,e_{kl}\left[\left(n_{ql}\left(k\right)\right)^q + \left(\bar{n}_{ql}\left(k\right)\right)^q\right]. \end{aligned} \tag{16}$$

If the energy density is defined by

$$\begin{aligned} \mathcal{E} &= \frac{1}{2}\,m_\sigma^2\left\langle\sigma\right\rangle^2 + \frac{1}{2}\,m_\delta^2\left\langle\delta_3\right\rangle^2 + \frac{1}{2}\,m_{\sigma^*}^2\left\langle\sigma^*\right\rangle^2 - \frac{1}{2}\,m_\omega^2\left\langle\omega_0\right\rangle^2 - \frac{1}{2}\,m_\rho^2\left\langle\rho_{03}\right\rangle^2 - \frac{1}{2}\,m_\phi^2\left\langle\phi_0\right\rangle^2 \\ &\quad + 2\sum_{\substack{B=p,n,\Lambda,\Sigma^+,\\ \Sigma^0,\Sigma^-,\Xi^0,\Xi^-}}\left\{\left(\int\frac{d^3\mathbf{k}}{(2\pi)^3}E_{kB}^*\left[\left(n_{qB}\left(k\right)\right)^q + \left(\bar{n}_{qB}\left(k\right)\right)^q\right]\right) + V_B\rho_B\right\} \\ &\quad + \sum_{l=e^-,\mu^-,\nu_e,\nu_\mu}\gamma_l\int\frac{d^3\mathbf{k}}{(2\pi)^3}\,e_{kl}\left[\left(n_{ql}\left(k\right)\right)^q + \left(\bar{n}_{ql}\left(k\right)\right)^q\right], \end{aligned} \tag{17}$$

Equation (16) is just the thermodynamic relation:

$$\Omega_q = \mathcal{E} - TS - \sum_{\substack{i=p,n,\Lambda,\Sigma^+,\Sigma^0,\Sigma^-,\\ \Xi^0,\Xi^-,e^-,\mu^-,\nu_e,\nu_\mu}}\mu_i\,\rho_i. \tag{18}$$

So as to obtain the normal expression of pressure

$$\begin{aligned} P &= -\,\Omega_q = \frac{2}{3}\sum_{\substack{B=p,n,\Lambda,\Sigma^+,\\ \Sigma^0,\Sigma^-,\Xi^0,\Xi^-}}\int\frac{d^3\mathbf{k}}{(2\pi)^3}\,\frac{k^2}{E_{kB}^*}\left[\left(n_{qB}\left(k\right)\right)^q + \left(\bar{n}_{qB}\left(k\right)\right)^q\right] \\ &\quad + \frac{1}{3}\sum_{l=e^-,\mu^-,\nu_e,\nu_\mu}\gamma_l\int\frac{d^3\mathbf{k}}{(2\pi)^3}\,\frac{k^2}{e_{kl}}\left[\left(n_{ql}\left(k\right)\right)^q + \left(\bar{n}_{ql}\left(k\right)\right)^q\right] \\ &\quad - \frac{1}{2}\,m_\sigma^2\left\langle\sigma\right\rangle^2 - \frac{1}{2}\,m_\delta^2\left\langle\delta_3\right\rangle^2 - \frac{1}{2}\,m_{\sigma^*}^2\left\langle\sigma^*\right\rangle^2 + \frac{1}{2}\,m_\omega^2\left\langle\omega_0\right\rangle^2 + \frac{1}{2}\,m_\rho^2\left\langle\rho_{03}\right\rangle^2 + \frac{1}{2}\,m_\phi^2\left\langle\phi_0\right\rangle^2, \end{aligned} \tag{19}$$

the power-law index has to satisfy the condition [15]:

$$1 < q < 4/3. \tag{20}$$

For baryons, electron and muon, the deformed Fermi integrals in Eqs. (11), (13), (15), (17) and (19) are transformed to the integrals in finite ranges by converting the variable k into $1/E^*_{kB}$ or $1/e_{kl}$. They are calculated in the adaptive automatic integration using 20-points Gaussian quadrature. The condition (20) also guarantees finite values of the integrals. For neutrinos the deformed Fermi integrals are calculated using the double exponential formula [17] for an integral in finite range. The upper limit of the variable k is determined so that the result is converged.

In our model the leptons are treated as the free Fermi gases. They however couple to baryons through the chemical equilibrium condition

$$\mu_i = b_i\,\mu_n - q_i\left(\mu_{e^-} - \mu_{\nu_e}\right), \tag{21}$$

$$\mu_{\mu^-} - \mu_{\nu_\mu} = \mu_{e^-} - \mu_{\nu_e}, \tag{22}$$

and the charge neutral condition

$$\sum_{i=p,\Sigma^+,\Sigma^-,\Xi^-,e^-,\mu^-} q_i\,\frac{\rho_i}{\rho_T} = 0, \tag{23}$$

and the lepton number conservation [1]

$$Y_{Le} = \frac{\rho_{e^-} + \rho_{\nu_e}}{\rho_T} = 0.4, \tag{24}$$

$$Y_{L\mu} = \frac{\rho_{\mu^-} + \rho_{\nu_\mu}}{\rho_T} = 0, \tag{25}$$

where b_i and q_i are baryon number and charge of each particle and ρ_T is the total baryon density

$$\rho_T = \sum_{\substack{B=p,n,\Lambda,\Sigma^+,\\ \Sigma^0,\Sigma^-,\Xi^0,\Xi^-}} \rho_B. \tag{26}$$

Then, for a definite value of ρ_T we solve 11-rank non-linear simultaneous equations of (5)-(10), (18) and (23)-(26) so that M^*_p, M^*_n, M^*_Λ, V_p, V_n, V_Λ, μ_n, μ_{e^-}, μ_{ν_e}, μ_{ν_μ} and T are determined. Using them the energy density (17) and the pressure density (19) are calculated. The results are the inputs to Tolman-Oppenheimer-Volkov equation [18]:

$$\frac{d\,M_G\,(r)}{d\,r} = \frac{4\,\pi^2}{c^2}\,r^2\,\mathcal{E}\,(r)\,, \tag{27}$$

$$\frac{d\,P\,(r)}{d\,r} = -\,\frac{G}{c^2}\,\frac{\left[\,\mathcal{E}(r) + P\,(r)\right]\left[M_G\,(r) + 4\,\pi\,r^3 P\,(r)/c^2\right]}{r\left[\,r - 2\,G M_G\,(r)/c^2\,\right]}. \tag{28}$$

$P\,(r)$, $\mathcal{E}\,(r)$ and $M_G\,(r)$ are the radial distributions of pressure, energy and gravitational mass of PNS.

Figure 1 shows the temperature profile in an isentropic core of PNS at the entropy per baryon $S = 1$. The black, red, blue and green curves are the results for $q = 1.0$, 1.1, 1.2 and 1.3, respectively. Because of the subextensivity [11] of the generalized entropy for $q > 1$, under a definite local entropy or a definite entropy per baryon, the total entropy of global system is lower as the power-law index is larger. Because the temperature is a constant for the global system or the uniform nuclear matter, it is lower as the global entropy is lower. The temperature therefore decreases as the power-law index increases. On the other hand, the global system with the long-ranged gravitational potential is ordered better than the system without gravitation even if we assume the same local entropy for both the system. The gravitation therefore leads to the subextensivity of the generalized entropy. Consequently, it is seen that the results in Fig. 1 reflect the effect of gravitation.

Figure 2 shows the particle fractions in an isentropic core of PNS at $S = 1$ within the standard Boltzmann-Gibbs thermo-statistics, while Fig. 3 shows them within the generalized thermo-statistics of $q = 1.3$. Among all the hyperons Λ appears first because it is the lightest one and because its potential in the saturated nuclear matter is assumed to be most attractive. (See Eq. (54) in Ref. [16].) Next, Ξs appear because their potential is also assumed to be attractive. The negatively charged Ξ^- appears earlier than the neutral Ξ^0 because of the charge neutrality of PNS. On the other hand, Σs are too scarce to be visible in the figures except for Σ^+ above $\rho_T = 0.95\mathrm{fm}^{-3}$ in Fig. 3. This is because Σ's potential in the saturated nuclear matter is assumed to be repulsive. The leptons μ^- and $\bar{\nu}_\mu$ are also too scarce to be visible because of the lepton number conservation (25).

The hyperons appear at lower baryon densities in Fig. 3 than Fig. 2. However, the particle fractions at $\rho_T = 1.0\mathrm{fm}^{-3}$ in Fig. 3 are almost the same as those in Fig. 2. The result suggests that EOS in the core of PNS is weakly dependent on a value of the power-law index. We can confirm the suggestion in Fig. 4, in which the black solid and red dashed curves show the EOSs in the standard ($q = 1.0$) and generalized ($q = 1.3$) thermo-statistics, respectively. There is little difference between the two EOSs. The result seems to be inconsistent with the result in Fig. 1, where the green curve is much lower than the black curve. It is however noted that the same local entropy or the same entropy per baryon leads us to almost the same EOS of PNS irrespective of the internal temperature. This is because the temperature is a constant inherent in global system while the EOS of PNS is developed in local micro-canonical nuclear system.

Next, we assume that the PNS has an isentropic core in the region $\rho_T \geq 0.1\mathrm{fm}^{-3}$

but a cold crust in the region $\rho_T < 10^{-3}\mathrm{fm}^{-3}$. For the former the EOSs in Fig. 4 are applied while for the latter we make use of the EOSs by Feynman-Metropolis-Teller, Baym-Pethick-Sutherland and Negele-Vautherin in Ref. [19]. The EOS between the two regions is obtained from simple linear interpolation. Figure 5 shows the mass-radius relation of PNS in the standard ($q = 1.0$) and generalized ($q = 1.3$) thermo-statistics. Because there is little difference between the two EOSs in Fig. 4, the difference between the black and red curves in Fig. 5 is also small. The most massive PNSs have the gravitational masses $M_G = 1.849M_\odot$ and $1.845M_\odot$, respectively. The corresponding radii are $R = 12.78$km and 12.69km, respectively. The corresponding central baryon densities are $\rho_T = 0.822\mathrm{fm}^{-3}$ and $0.826\mathrm{fm}^{-3}$, respectively. However, we still see a clear difference between the standard and generalized thermo-statistics in Fig. 5. The difference should be due to much lower temperature of the green curve than the black curve in Fig. 1. It has been also shown in the analysis of Fig. 1 that the lower temperature is due to the effect of gravitation. Consequently, Fig. 5 clearly shows the effect of gravitation on PNS in the generalized thermo-statistics, although an extreme case of $q = 1.3$ is only a numerical experiment that is unlikely to be physically realized.

We have calculated PNS for the first time in the generalized thermo-statistics. Because the EOS of PNS matter is developed in local micro-canonical nuclear system, under a definite entropy per baryon the dependence of EOS on the power-law index is weak. However, the subextensive entropy for $q > 1$ leads to much lower temperature in a core of PNS than the Clausius extensive entropy. As the result, we can see a small but clear difference between the mass-radius relation of PNS in an extreme case $q = 1.3$ and the standard thermo-statistics. Because the subextensivity is due to gravitation, it is concluded that the gravitation has an effect on the properties of PNS through the EOS developed in the generalized thermo-statistics.

References

[1] M. Prakash, I. Bombaci, M. Prakash, P.J. Ellis, R. Knorren and J.M. Lattimer, Phys. Rep. **280** (1997) 1, [arXiv:nucl-th/9603042].

[2] M. Prakash, J.M. Lattimer, J.A. Pons, A.W. Steiner and S. Reddy, Lect. Notes Phys. **578** (2001) 364 [arXiv:astro-ph/0012136].

[3] J.A. Pons, S. Reddy, M. Prakash, J.M. Lattimer and J.A. Miralles, Astrophys. J. **513** (1999) 780.

[4] K. Strobel, Ch. Schaab and M.K. Weigel, Astron. Astrophys. **350** (1999) 497.

[5] K. Strobel and M.K. Weigel, Astron. Astrophys. **367** (2001) 582.

[6] J.A. Pons, S. Reddy, P.J. Ellis, M. Prakash, and J.M. Lattimer, Phys. Rev. C **62** (2000) 035803 [arXiv:nucl-th/0003008].

[7] R. Mańka, M. Zastawny-Kubica, A. Brzezina and I. Bednarek, J. Phys. G **27** (2001) 1917 [arXiv:astro-ph/0012088].

[8] G.F. Marranghello, C.A.Z. Vasconcellos, M. Dillig and J.A. de F. Pacheco, Int. J. Mod. Phys. E **11** (2002) 83 [arXiv:astro-ph/0107476].

[9] D.P. Menezes and C. Providencia, Phys. Rev. C **69** (2004) 045801 [arXiv:nucl-th/0312050].

[10] O.E. Nicotra, M. Baldo, G.F. Burgio and H.-J. Schultz, Astron. Astrophys. **451** (2006) 213.

[11] C. Tsallis, Braz. J. Phys. **29** (1999) 1.

[12] Europhysics News **36** (2005) No.6 [http://www.europhysicsnews.com].

[13] C. Tsallis, http://tsallis.cat.cbpf.br/TEMUCO3.pdf.

[14] K. Miyazaki, Mathematical Physics Preprint Archive (mp_arc) 05-427.

[15] K. Miyazaki, Mathematical Physics Preprint Archive (mp_arc) 07-92.

[16] K. Miyazaki, Mathematical Physics Preprint Archive (mp_arc) 06-175.

[17] http://www.kurims.kyoto-u.ac.jp/~oura/intde-j.html

[18] W.D. Arnett and R.L. Bowers, Astrophys. J. Suppl. **33** (1977) 415.

[19] V. Canuto, Ann. Rev. Astr. Ap. **12** (1974) 167; **13** (1975) 335.

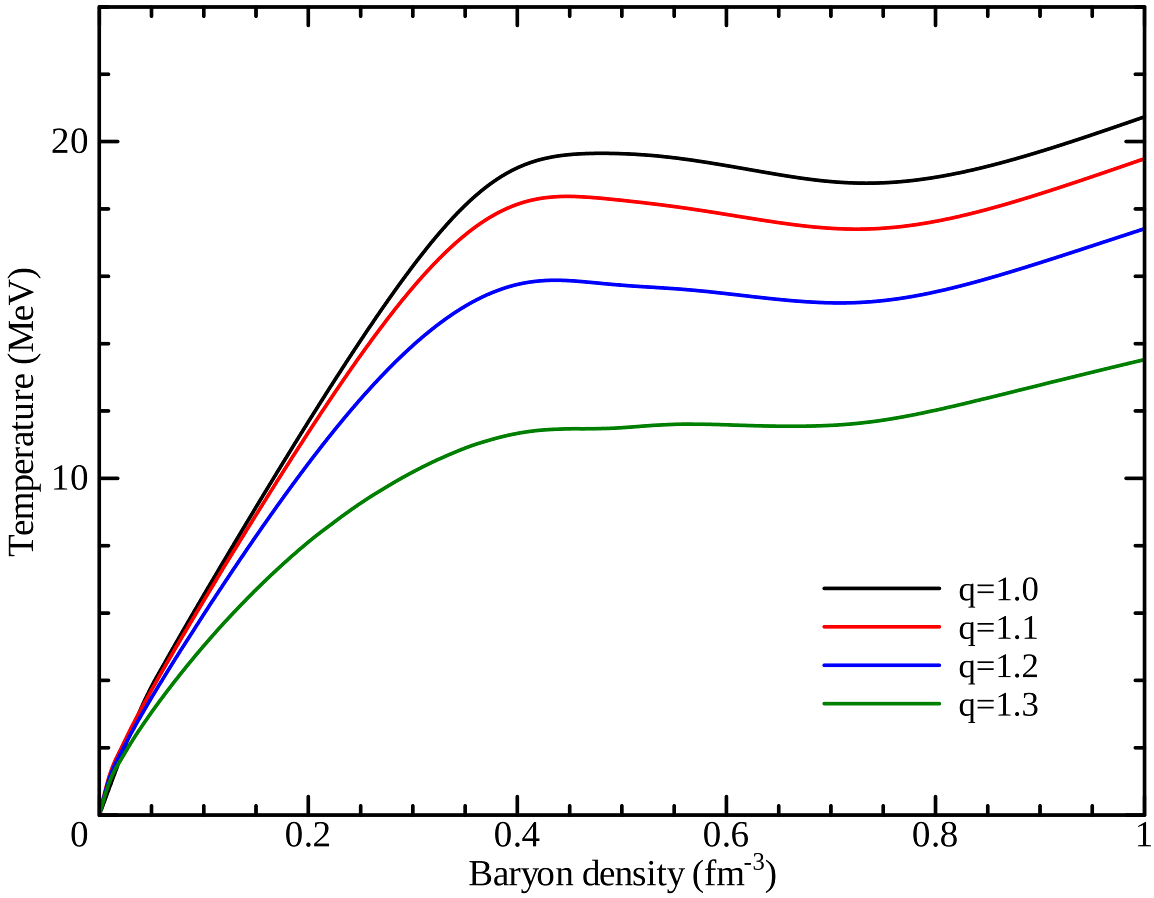

Figure 1: The temperature profile in an isentropic core of PNS at the entropy per baryon $S = 1$ for $q = 1.0$, 1.1, 1.2 and 1.3, respectively.

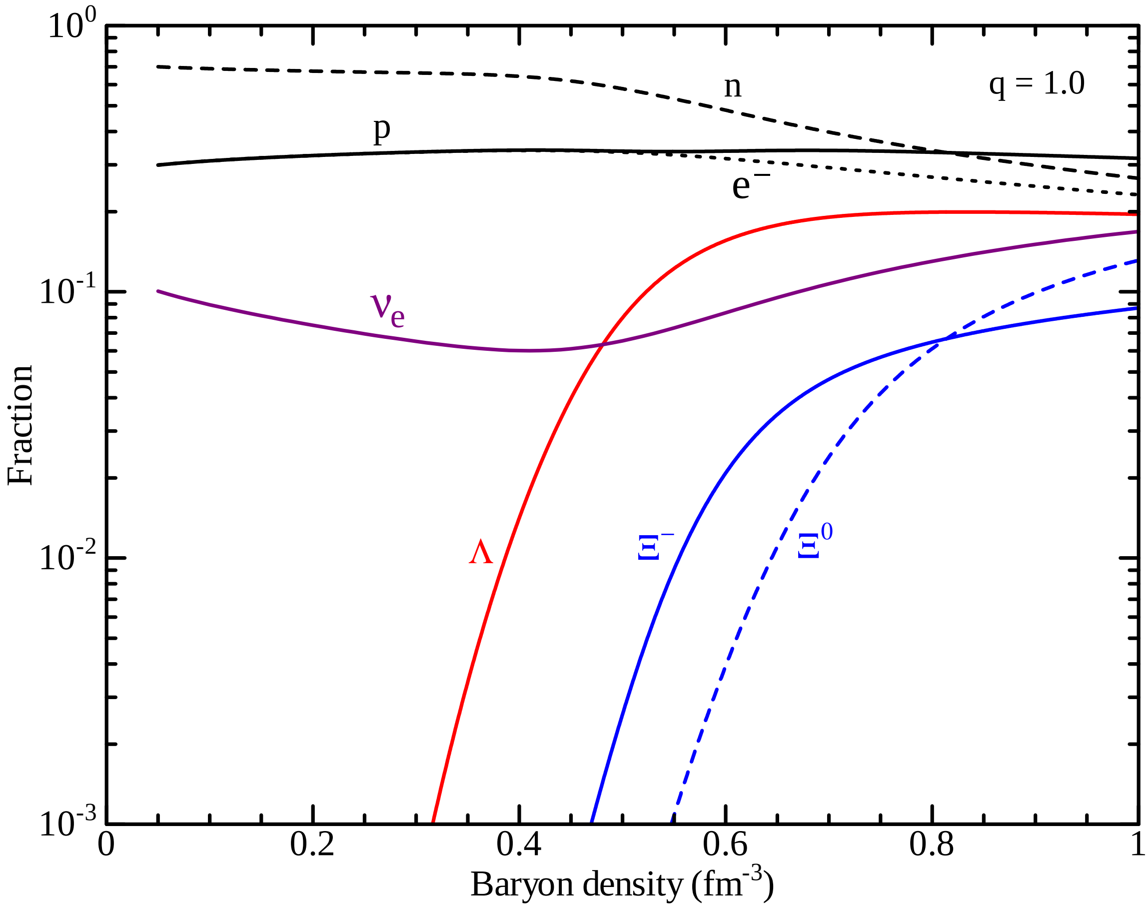

Figure 2: The particle fractions in an isentropic core of PNS at the entropy per baryon $S = 1$ in the standard Boltzmann-Gibbs thermo-statistics.

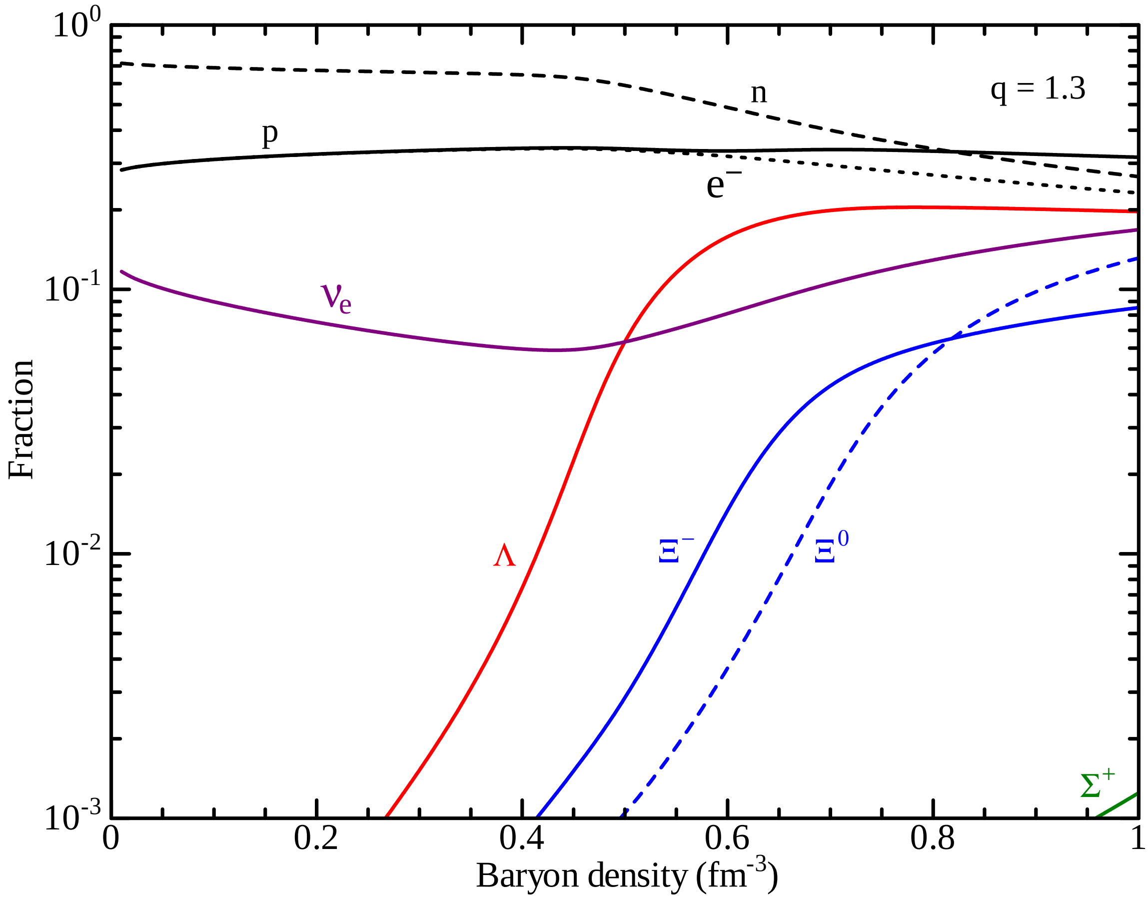

Figure 3: The particle fractions in an isentropic core of PNS at the entropy per baryon $S = 1$ in the generalized thermo-statistics of $q = 1.3$.

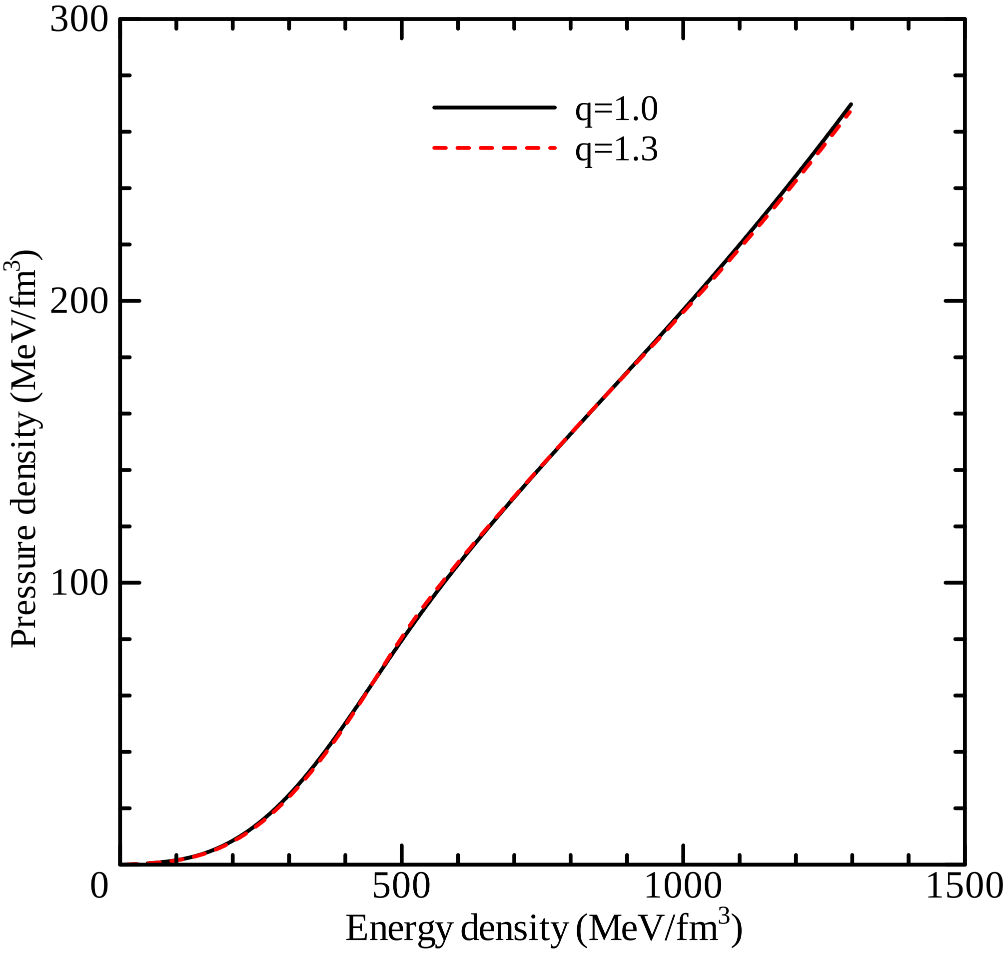

Figure 4: The equation-of-state for the isentropic core of PNS at the entropy per baryon $S = 1$ in the standard ($q = 1.0$) and generalized ($q = 1.3$) thermo-statistics.

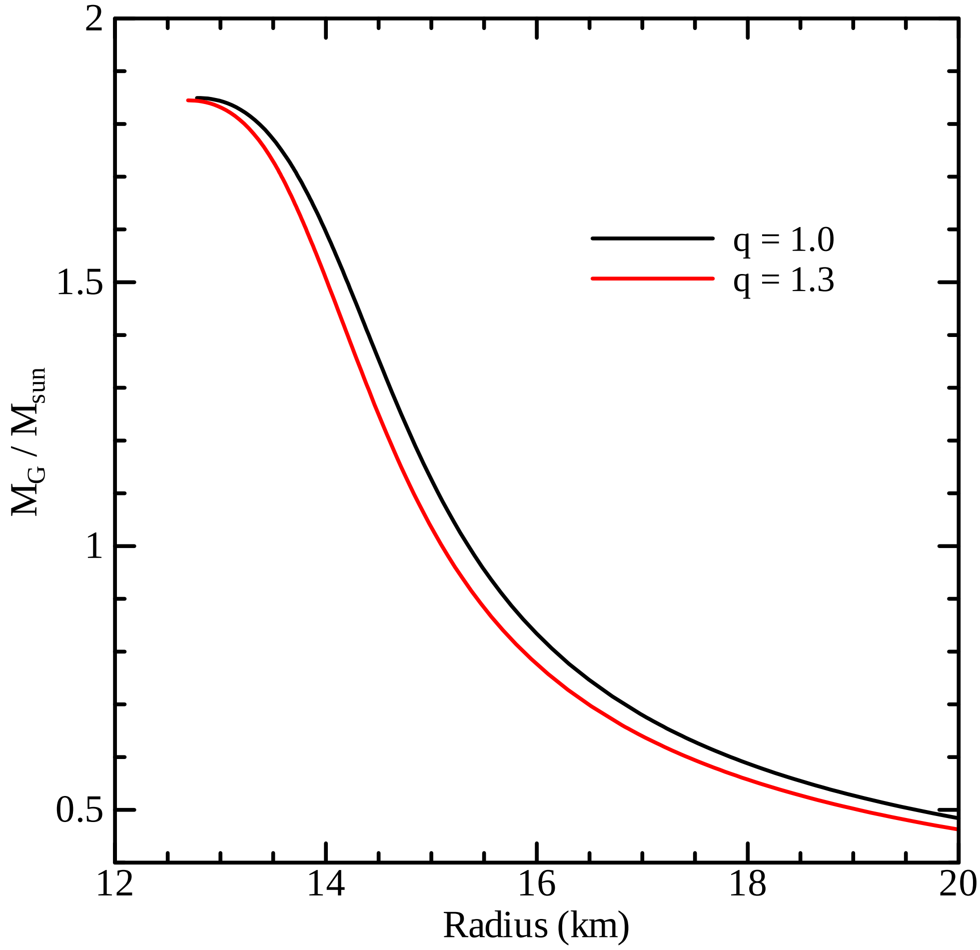

Figure 5: The mass-radius relation of PNS in the standard ($q = 1.0$) and generalized ($q = 1.3$) thermo-statistics.